# Methods for mapping mechanisms to developable surfaces

# Lance P. Hyatt\*, Jacob R. Greenwood, Jared J. Butler, Spencer P. Magleby and Larry L. Howell

Department of Mechanical Engineering, Brigham Young University, 350 EB, Provo UT 84602, Utah, USA

Email: lance.hyatt@byu.edu

Email: jacobgwood@gmail.com

Email: butler@psu.edu
Email: magleby@byu.edu
Email: lhowell@byu.edu
\*Corresponding author

Abstract: Planar and spherical mechanisms can be mapped to regular cylindrical and circular conical developable surfaces using cyclic quadrilaterals. The link lengths and link angles can be used in equations to calculate the circumcircle of a cyclic quadrilateral to find the radius or cone angle of a developable surface. Two other numerical and graphical methods to map mechanisms to these surfaces are discussed and expanded. Useful properties of developable mechanisms are also identified using cyclic quadrilaterals. While Grashof mechanisms can be mapped to developable surfaces in either their open or crossed configurations, the only way to map a non-Grashof mechanism to a cylindrical or conical surface is in its open configuration. Extramobile and intramobile behaviour can be predicted based the cyclic quadrilateral's position within the circumcircle and the mechanism's grounded link. The possible configurations are tabulated and analysed.

**Keywords:** developable mechanisms; kinematics; cyclic quadrilaterals; cylinder; cone.

**Reference** to this paper should be made as follows: Hyatt, L.P., Greenwood, J.R., Butler, J.J., Magleby, S.P. and Howell, L.L. (2021) 'Methods for mapping mechanisms to developable surfaces', *Int. J. Mechanisms and Robotic Systems*, Vol. 5, Nos. 1/2, pp.39–60.

**Biographical notes:** Lance P. Hyatt recently graduated with a Master's degree from the Brigham Young University where his research focused on developable mechanisms. He is currently a PhD student at the Penn State University.

Jacob R. Greenwood is a recent Master's graduate from the Brigham Young University where his research focused on developable mechanisms and origami-based engineering design.

Jared J. Butler is currently an Assistant Professor at the Penn State University. His research focuses include compliant and deployable mechanisms.

Spencer P. Magleby is the Director of the University Honors Program and a Professor at the Brigham Young University. His research is aimed at improving the processes and tools of engineering design and technology development with a focus on mechanical systems, compliant mechanisms, product design and collaboration.

Larry L. Howell is an Associate Academic Vice President and a Professor at the Brigham Young University. His research focuses on compliant mechanisms, including origami-inspired mechanisms, space mechanisms, microelectromechanical systems, and medical devices.

This paper is a revised and expanded version of a paper entitled 'Using cyclic quadrilaterals to design cylindrical developable mechanisms' presented at Proceedings of the 2020 USCToMM Mechanical Systems and Robotics Symposium, Rapid City, South Dakota, 14–16 May 2020.

#### 1 Introduction

Developable surfaces (e.g., generalised cylinders, generalised cones, and tangent developed surfaces) are common in many engineering applications (Lawrence, 2011; Liu et al., 2011; Martín-Pastor, 2019; Lim and Erdman, 2003; Gavriil et al., 2019; Caymaz et al., 2018). Developable mechanisms are mechanisms that conform to the shape of developable surfaces (Nelson et al., 2019). These mechanisms are advantageous because they can be incorporated into the surface of an object, allowing for compact storage and precise deployed motion. For example, Seymour et al. (2019) outlined several applications in minimally invasive surgery where a complex mechanism can be embedded in the cylindrical shaft of surgical tools. When the tool is inserted into a small incision, the compact mechanism can expand to perform additional functions.

While developable mechanisms provide unique advantages, they can be difficult to design. To conform to a developable surface, the joint axes must align with the ruling lines, and the links must be shaped to fit within the surface (Nelson et al., 2019). Methods have been proposed for designing and analysing developable mechanisms on regular cylindrical (Greenwood et al., 2019) and circular conical (Hyatt et al., 2020) surfaces.

One specific difficulty to designing developable mechanisms is knowing how to map a given mechanism onto a developable surface to create a developable mechanism. For cylindrical and conical developable mechanisms, this means finding the geometry of the surface (the radius of a cylindrical surface or cone angle of a conical surface) where a mechanism will fit and the configuration of the mechanism when conformed to the surface.

This paper introduces three methods for mapping four-bar linkages to cylindrical and conical developable surfaces and is organised as follows. First, a mapping method based on cyclic quadrilaterals is presented. Second, two additional mapping methods are introduced, both of which are expansions of previous work in the field. These methods are expanded to apply to both cylinders and cones. Next, the cyclic

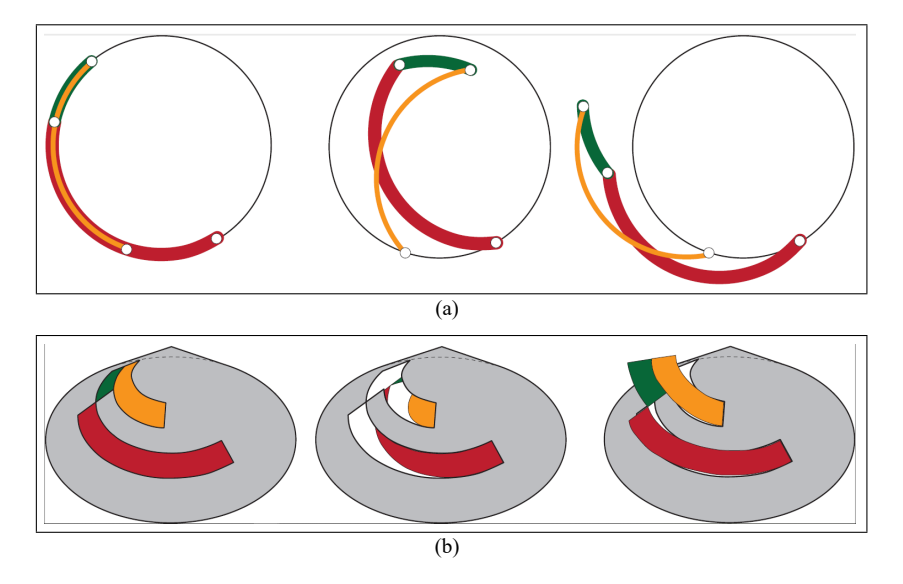
quadrilaterals mapping method is applied to analyse the behaviour of cylindrical and conical developable mechanisms. The final section includes a discussion of the results.

### 2 Background

# 2.1 Developable mechanisms

Developable mechanisms are mechanisms that are contained within or conform to developable surfaces (Nelson et al., 2019). Their design can be more complex than traditional mechanisms because they need to take into account the shape and position of the developable surface (Nelson et al., 2019; Greenwood et al., 2019). Mechanisms can be mapped to these different surfaces by aligning the joints of a mechanism to the surface's ruling lines. Specifically, planar mechanisms can be mapped to cylindrical surfaces as all of the joint axes are parallel, and a spherical mechanisms can be mapped to conical surfaces as all of the joint axes intersect at a single point. The links are shaped so that the mechanism conforms to the surface.

Figure 1 An example of a, (a) cylindrical (b) conical developable mechanism that show both intramobile and extramobile behaviour (see online version for colours)



Notes: The left shows the mechanisms in their conformed position, the centre shows all of the links moving within the surface (intramobile), and the right shows all of the links moving outside the surface (extramobile).

Greenwood et al. (2019) defined three types of behaviours that developable mechanisms can exhibit as they move from their conformed position: extramobile (all parts of the linkage move outside the reference surface), intramobile (all parts of the linkage move inside the reference surface), and transmobile (the linkage has parts that move both inside and outside the reference surface). Extramobile and intramobile behaviours are of particular interest as they present motion that allows for mechanisms that move

purely into or away from the surface. Figure 1 shows examples of a cylindrical and a conical developable mechanism, each of which exhibit both extramobile and intramobile behaviour. Other work has also explored the limits of intramobile and extramobile motion for cylindrical developable mechanisms Butler et al. (2020).

#### 2.2 Grashof condition

The Grashof criterion classifies the relative motion of links in a four-bar mechanism. For a Grashof mechanism, at least one link of a four-bar mechanism can rotate completely with respect to the other links (Grashof, 1883). The traditional equations are shown below in Table 1, where the shortest and longest links are labeled as s and l, respectively and the other two links are p and q.

**Table 1** Two analytical methods for determining the Grashof condition of four-bar mechanisms

Traditional eq.	McCarthy's eq.	Grashof criteria				
$s+l \le p+q$	$T_1 T_2 T_3 \ge 0$	Grashof mechanism				
s+l > p+q	$T_1 T_2 T_3 < 0$	non-Grashof mechanism				
s+l=p+q	$T_1 T_2 T_3 = 0$	folding mechanism (special case Grashof)				

McCarthy and Soh (2010) used three different parameters to determine the Grashof condition for planar mechanisms. Given a mechanism with links (a, b, c, d), the parameters  $T_1$ ,  $T_2$ , and  $T_3$  are defined below. The product of these three parameters can determine the Grashof condition, as shown in Table 1.

$$T_1 = a + b - c - d \tag{1}$$

$$T_2 = a - b + c - d \tag{2}$$

$$T_3 = -a + b + c - d \tag{3}$$

McCarthy also presented similar parameters to determine the Grashof condition for spherical mechanisms using the link angles instead of link lengths.

#### 2.3 Cyclic quadrilaterals

A cyclic quadrilateral is a quadrilateral whose four vertices all lie on a single circle, called the circumcircle (Usiskin, 2008; Andreescu and Enescu, 2011). The properties of these quadrilaterals continue to be studied extensively in mathematical research (Fraivert et al., 2019; Josefsson, 2019). Both convex and crossed cyclic quadrilaterals are possible (Josefsson, 2017), as shown in Figure 2.

Gupta (1977) showed that any set of four lines (a, b, c, d) can form a convex cyclic quadrilateral of radius R as long as the longest line is shorter than the sum of the other three lines, where R is

$$R = \frac{1}{4} \sqrt{\frac{(ab+cd)(ac+bd)(ad+bc)}{(s-a)(s-b)(s-c)(s-d)}}$$
 (4)

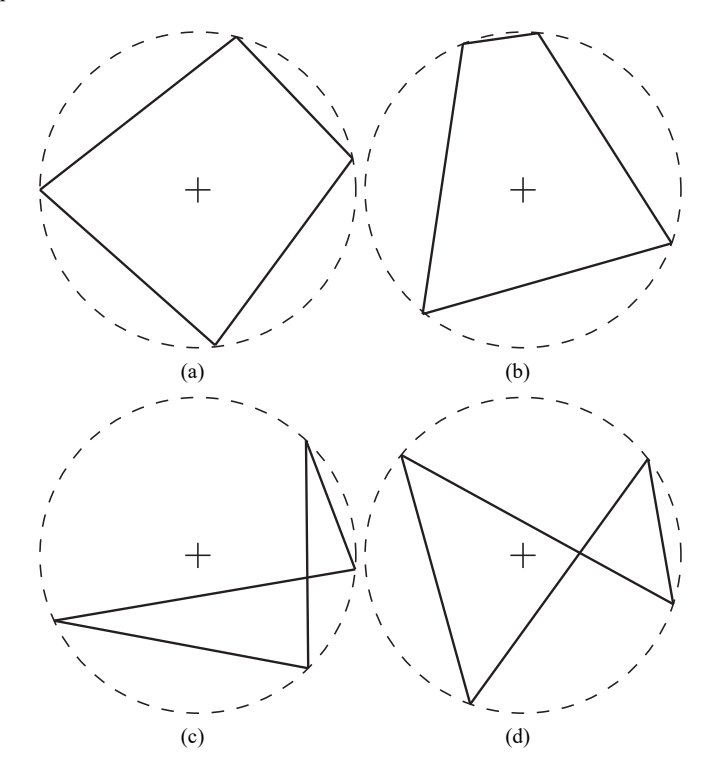
where

$$s = \frac{a+b+c+d}{2}$$

Josefsson (2017) provided a similar equation for crossed cyclic quadrilaterals, using

$$R = \sqrt{\frac{(ab - cd)(ac - bd)(ad - bc)}{(-a + b + c - d)(a - b + c - d)(a + b - c - d)(a + b + c + d)}}$$
 (5)

Figure 2 (a) (b) Examples of convex cyclic quadrilaterals (c) (d) Examples of crossed cyclic quadrilaterals



# 2.4 Existing methods to map four-bar mechanisms to developable surfaces

Two methods have been presented in the literature for mapping four-bar mechanisms to developable surfaces. These are briefly reviewed here and are later expanded to cover both cylindrical and conical surfaces.

#### 2.4.1 Coordinate method for cylindrical developable mechanisms

Murray and McCarthy (2020) presented an analytical method using normalised coordinate positions for mapping a planar linkage to a cylindrical surface. The method,

used for cylindrical developable mechanisms, normalises the link lengths so that the grounded link has a value of 1. Then, by assigning coordinate values to each joint location, the constraint of each point being located on a circle is applied. This results in a system of six equations, as shown below, where (g, a, h, b) are normalised link lengths of a given four-bar mechanism and g = 1.

$$x_1y_2 + x_2y_1 + b^2y_1 - a^2y_2 = 0$$

$$1 + x_2 - x_1 - x_3 = 0$$

$$y_2 - y_1 - y_3 = 0$$

$$x_1^2 + y_1^2 - a^2 = 0$$

$$x_2^2 + y_2^2 - b^2 = 0$$

$$x_3^2 + y_3^2 - h^2 = 0$$
(6)

The parameters  $(x_1, y_1, x_2, y_2, x_3, y_2)$  are the six unknown coordinates that can be found with a numerical solver then used find the centre of the circle K and the radius R.

$$K = \frac{b^2 + x_2}{2y_2} \tag{7}$$

$$R^2 = (1/2)^2 + K^2 \tag{8}$$

#### 2.4.2 Loop sum method for conical developable mechanisms

Hyatt et al. (2020) presented the loop sum method for determining the cone angle needed to map a given spherical mechanism to a conical surface. This method uses the properties of the planar projection of the link angles of a conical mechanism to develop a set of 16 equations as functions of an unknown cone angle. Through numerical or graphical analysis, the correct cone angle can be found, as shown below.

Conical developable mechanisms can be represented by a projecting the curved links onto a planar cross-section of the conical surface. For this method, the projected angles [the angles of rotation between the vertices as seen in Figure 3(a)] are used to find the unknown cone angle. For a spherical link angle  $\phi$ , the projected angle  $\phi_0$  for a conical surface with a cone angle of  $\lambda$  is

$$\phi_0 = \cos^{-1} \left( \frac{\cos \alpha - \sin^2(\lambda)}{\cos^2(\lambda)} \right) \tag{9}$$

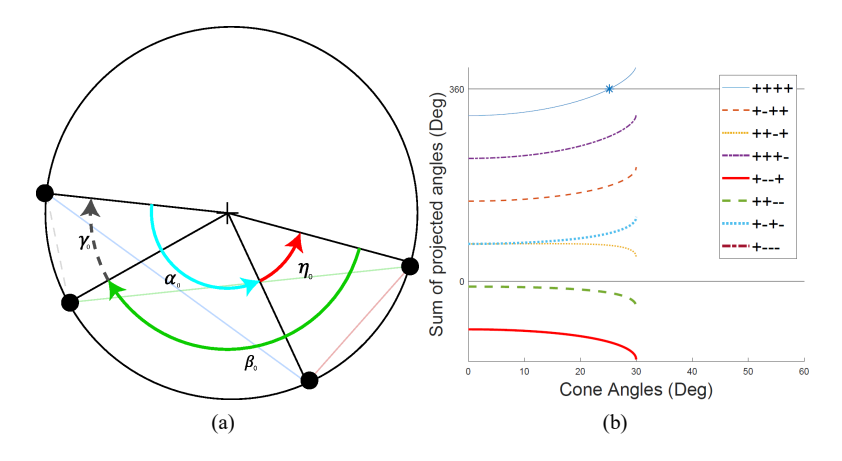
The projected angles will always sum to an integer multiple of  $360^{\circ}$ . Note that the projected angle in equation (9) can be either positive or negative. Therefore, for a spherical mechanism with link angles  $(\gamma, \alpha, \eta, \beta)$  and projected angles  $(\gamma_0, \alpha_0, \eta_0, \beta_0)$  the following relationship is found.

$$\pm \gamma_0 \pm \alpha_0 \pm \eta_0 \pm \beta_0 = 360k \tag{10}$$

where k is an integer.

Equation (10) yields 16 different combinations of different signs of angles that can be plotted as functions of  $\lambda$ . If, at some cone angle, one of the equations is equal to a multiple of 360, that indicates the angle of the conical surface to which the spherical mechanism can be mapped. This is demonstrated for a spherical mechanism with link angles (70°, 80°, 120°, 40°). Figure 3(b) shows eight of the combinations, and in this example only the combination with the signs (++++) crosses the value 360 indicating a cone angle of about 25.21°. The eight excluded equations are mirrored about the horizontal axis.

Figure 3 (a) Projected angles on a cross-section of a conical developable mechanism (b) Eight combinations of projected angles for a non-Grashof mechanism (see online version for colours)



Note: One combination crosses a multiple of 360 indicating a valid cone angle.

#### 3 Mapping method using cyclic quadrilaterals

This section introduces how cyclic quadrilaterals can be used to map planar and spherical linkages to cylindrical and conical developable surfaces. Using cyclic quadrilaterals to represent a four-bar mechanism whose joints lie on a circle yields useful insights to both cylindrical and conical developable mechanism design.

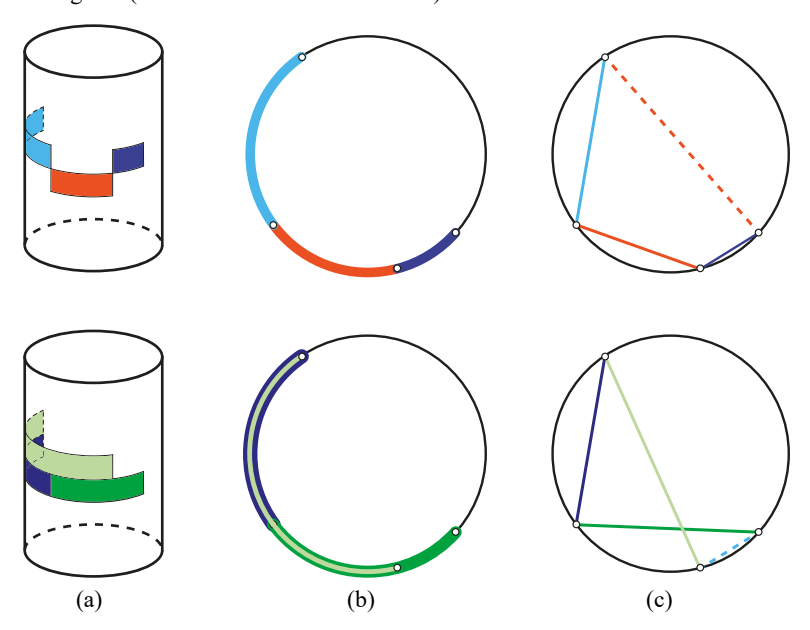
#### 3.1 Cylindrical developable mechanisms

The links of cylindrical developable mechanisms have the same curvature as the cylindrical reference surface. However, the shape of the links does not affect the kinematic analysis, which only relies on the relative position of the joints (Gupta, 1977). Therefore, when performing kinematic analysis, the curved links can be represented by a skeleton diagram, straight lines connecting the joint axes.

For a four-bar developable mechanism on a regular cylindrical surface, the skeleton diagram will be a cyclic quadrilateral. The sides of the quadrilateral are the links of the mechanism, the vertices are the joints, and the circumcircle is a cross-section of

the cylindrical reference circle. Hence, four-bar cylindrical developable mechanisms can be represented by cyclic quadrilaterals, either convex or crossed. Figure 4 shows an example of this relationship.

Figure 4 (a) Two cylindrical developable mechanisms (b) With a cross-section (c) Skeleton diagram (see online version for colours)



Notes: The mechanism on the top is in its open configuration, and the bottom mechanism is in a crossed configuration.

The dashed line indicates the grounded link.

This section will discuss cyclic quadrilaterals and their application to four-bar cylindrical developable mechanisms. The convex case will be discussed first, followed by the crossed case, and the special case of a folding mechanism. These results lead to a generalised equation that relates the link lengths and cyclic quadrilateral configuration to the radius of the cylindrical reference surface.

#### 3.1.1 Convex cyclic quadrilaterals

The convex cyclic position represents the mechanism's open circuit. Paramesvara's equation [equation (4)] shows that any set of four link lengths can form a convex cyclic quadrilateral (provided they can be assembled). This confirms what Bowman (1952) found, that all four-bar linkages have a possible convex cyclic position. Interestingly, the order in which the links are arranged (abcd or abdc or adbc) does not affect the radius of the reference circle (Bowman, 1952), as long as the mechanisms are in the open circuit.

# 3.1.2 Crossed cyclic quadrilaterals

The crossed cyclic position represents the mechanism's crossed circuit. Crossed cyclic quadrilaterals are possible and Josefsson provided an equation for their circumcircle [equation (5)]. While any four-bar mechanism can be in the convex cyclic position, only Grashof mechanisms can be in the crossed cyclic position, as shown below.

Brahmagupta developed a well-known equation for the area of a convex cyclic quadrilateral (Atzema, 2015) and Josefsson (2017) derived a similar equation for the area of a crossed cyclic quadrilateral given by

$$K = \frac{1}{4}\sqrt{(P_1)(P_2)(P_3)(P_4)} \tag{11}$$

where

$$P_1 = -a + b + c - d$$

$$P_2 = a - b + c - d$$

$$P_3 = a + b - c - d$$

$$P_4 = a + b + c + d$$

The parameters  $P_1$ ,  $P_2$ , and  $P_3$  are equivalent to the parameters  $T_3$ ,  $T_2$ , and  $T_1$  used by McCarthy and Soh (2010) to determine the Grashof condition (see Subsection 2.2). Links cannot have a negative length, so parameter  $P_4$  is always positive.

Assuming that a non-Grashof mechanism  $(P_1P_2P_3 < 0)$  can be in the crossed cyclic position, the product  $P_1P_2P_3P_4$  must be negative. When applied to equation (11), the resulting area is a complex number, which is impossible to physically make. Therefore, a non-Grashof mechanism does not have a crossed cyclic configuration.

#### 3.1.3 Special case: folding mechanism

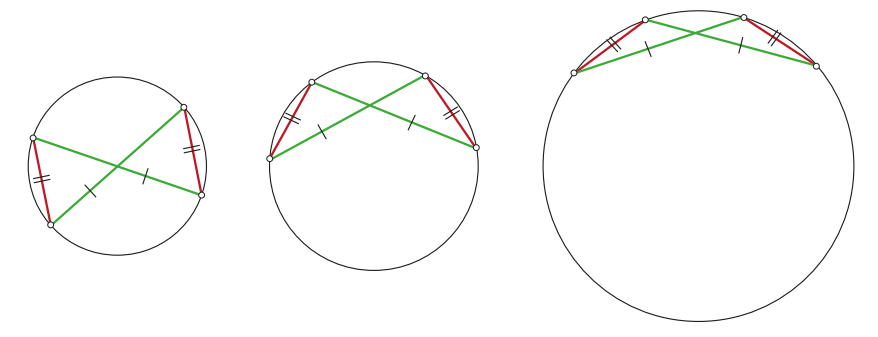
A folding, or change point mechanism ( $T_1T_2T_3 = 0$ ) is a mechanism where all links can be simultaneously colinear. It is a special-case Grashof mechanism and can therefore have positions in both the open and crossed circuits without disassembly.

Equation (4) can be used to find the radius of the circumcircle for the set of links when in an open circuit. However, when the mechanism is in its crossed configuration, equation (11), shows that  $P_1P_2P_3=0$ , resulting in an area of zero. This suggests that folding mechanisms in the crossed configuration can only conform to a circumcircle of infinite radius (i.e., all the links lie in a single line).

There are only two known cases where a crossed configuration of folding mechanism has a non-infinite radius. The first case is a parallelogram folding mechanism where opposite links have equal length. Parallelogram mechanisms in the crossed configuration can exist on a wide range of circumcircle radii. The range is from half the length of the longest link, l, to infinity ( $l/2 \le R < \infty$ ). An example of a parallelogram mechanism in several crossed cyclic configurations is shown in Figure 5. The second case is a kite mechanism with two sets of adjacent links with equal length. The crossed configuration of a kite mechanism is a special case where the equal adjacent links are stacked. The resulting skeleton diagram appears as two line segments because the links with equal length are coincident. This crossed or stacked configuration has the same range of

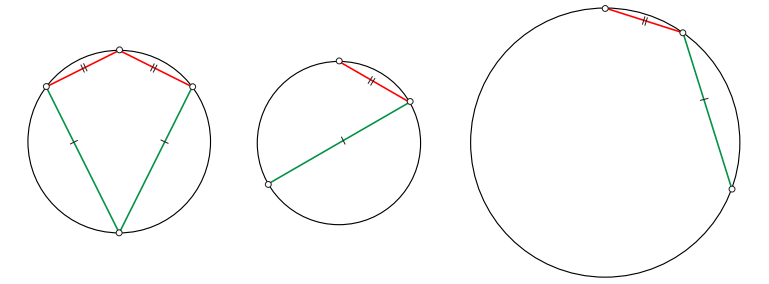
radii as the parallelogram mechanism. The open and stacked configurations of a kite mechanism are shown in Figure 6.

Figure 5 A folding mechanism with the green links equal and the red links equal (see online version for colours)



Notes: As a parallelogram mechanism, the same set of links can be circumscribed by circles of increasing radius as the mechanism approaches its folded position.

**Figure 6** A kite mechanism with the green links equal and the red links equal (see online version for colours)



Notes: The mechanism is shown in its open configuration (left) and two examples of its stacked configuration.

#### 3.1.4 Generalised equation for the radius of the circumcircle

Equations (4) and (5) are very similar, with the only changes dealing with the sign changes for d (Josefsson, 2017). Hence, these equations can be combined to design four-bar cylindrical developable mechanisms in both open and crossed configurations. This combination introduces a variable  $(\mu)$  that takes into account this sign change and corresponds to the circuit of the mechanism. The equation for the radius of the cylindrical reference surface R is

$$R = \frac{1}{4} \sqrt{\frac{(ab + \mu cd)(ac + \mu bd)(\mu ad + bc)}{(p - a)(p - b)(p - c)(p - \mu d)}}$$
(12)

where

$$p = \frac{a+b+c+\mu d}{2}$$

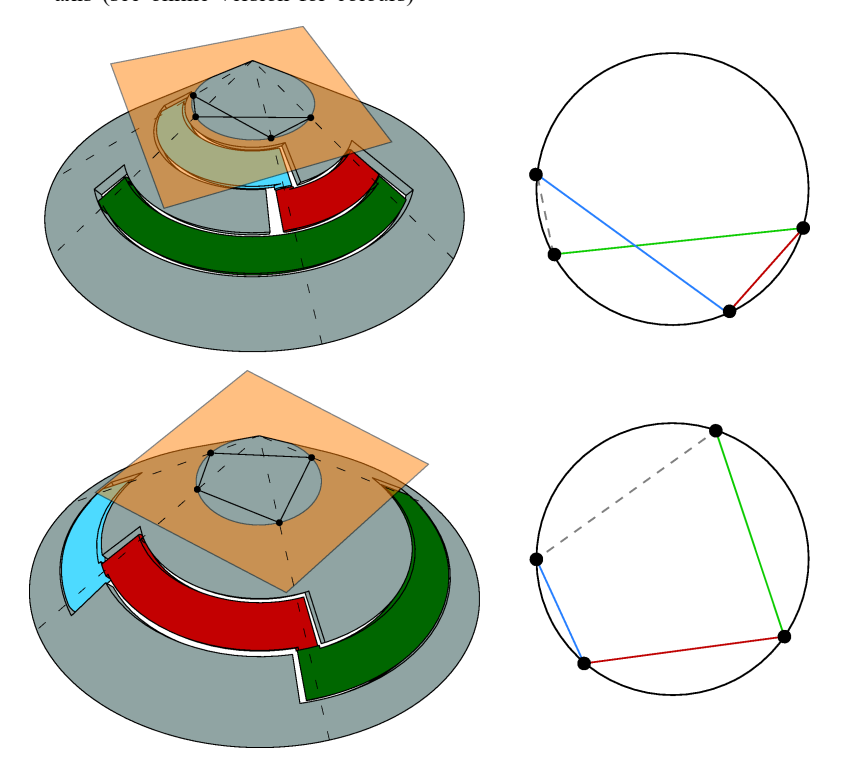
$$\mu = \begin{cases} 1 & \text{for an open configuration} \\ -1 & \text{for a crossed configuration} \end{cases}$$

This equation is valid for any Grashof mechanism, regardless of its circuit. However, as discussed above, it is not valid for non-Grashof mechanisms in the crossed circuit. For folding mechanisms, equation (12) may yield misleading results for the crossed configuration. The equation will correctly identify a solution with an infinite radius (a straight line), but as discussed in Subsection 3.1.3, some mechanisms may have multiple solutions.

#### 3.2 Conical developable mechanisms

Conical developable mechanisms are spherical mechanisms whose joint axes are aligned with the ruling lines of a conical surface and intersect at the apex of the cone. Instead of link lengths, spherical mechanisms are defined by link angles between adjacent joint axes. The links of conical developable mechanisms are curved to match the conical reference surface in the conformed position.

Figure 7 Two examples of conical mechanisms with an intersecting plane normal to the cone axis (see online version for colours)



Notes: If the points where the joint axes intersect with the plane are connected, a crossed (top) or open (bottom) cyclic quadrilateral can be formed.

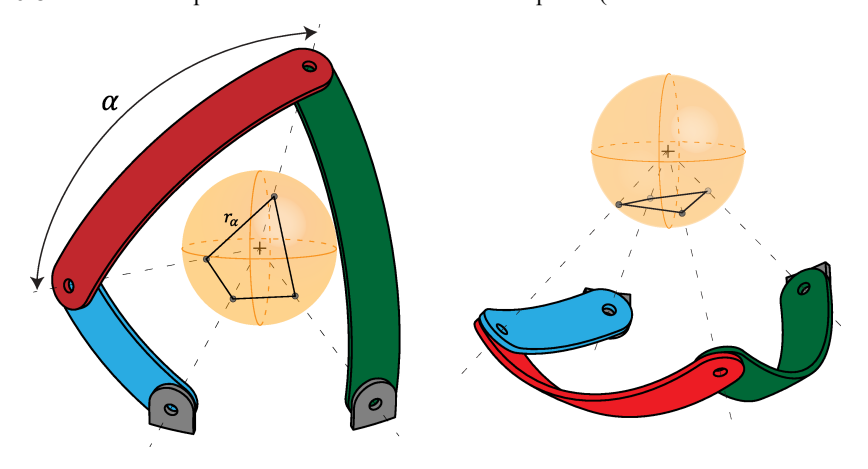
Similar to what was discussed in Subsection 3.1 on cylindrical developable mechanisms, straight lines may be used to represent the kinematic behaviour of these curved links. Previous work has shown that a developable mechanism on a circular conical surface can be represented by a two-dimensional cross-section (Hyatt et al., 2020). If a plane normal to the cone axis of a circular cone intersects with the surface, the resulting cross-section is a circle. For a four-bar developable mechanism on that surface, the joint axes intersect the resulting circle at four points equidistant from the apex of the cone. By connecting these four points in the same manner the links connect the joint axes, a cyclic quadrilateral is formed. The same process can be completed for any four-bar developable mechanism on a circular conical surface. Figure 7 shows examples of two conical mechanisms and the cyclic quadrilateral formed from the cross-section.

This section explores how cyclic quadrilaterals can be used to determine the geometry of a reference cone to which a spherical mechanism can be mapped. It is important to note that while the planar four-bar representation can be useful to determine how a conical developable mechanism behaves when moving from the conformed position, it does not represent the full three-dimensional motion. This is explored more in Subsection 3.2.3.

### 3.2.1 Visualising spherical mechanisms using a unit sphere

The joint axes of a spherical mechanism all intersect at a single point which causes the mechanism to move completely within a spherical surface (Chiang, 2000). If the relative angles between the joint axes do not change, the distance away from the centre of the sphere along the axes will not change the behaviour of the mechanism. Therefore, it is common to use a unit sphere to visualise and analyse mechanisms. Using the unit sphere also simplifies the following expressions.

Figure 8 A four-bar spherical mechanism and the unit sphere (see online version for colours)



Notes: By connecting the points where the joint axes intersect the sphere, a three-dimensional quadrilateral is formed.

With the four link angles of a spherical four-bar mechanism, a three-dimensional quadrilateral can be generated by connecting each joint axis with a straight line at

the point the axis intersects with the unit reference sphere. Figure 8 shows a four-bar spherical mechanism and the resulting three-dimensional quadrilateral. Given a link angle  $\alpha$ , the length of one side of the quadrilateral  $r_{\alpha}$  is

$$r_{\alpha} = \sqrt{2 - 2\cos(\alpha)} \tag{13}$$

# 3.2.2 Calculating the cyclic quadrilateral geometry

To conform to a circular cone, there must be a configuration of the three-dimensional quadrilateral that lies on a single plane creating a cyclic quadrilateral. Gupta (1977) proved that if no one link is greater than the sum of the other links, a cyclic quadrilateral can be formed. If the lengths of the three-dimensional quadrilateral satisfy that condition, equation (12) can be used to find the radius of the circumcircle of the convex or crossed cyclic quadrilateral. The resulting circumcircle can be considered as a cross-section of a circular cone. The vertices of the quadrilateral lie on a conical surface whose apex coincides with the centre of the unit sphere. The cone angle of the conical surface,  $\lambda$ , is the inverse cosine of the radius of the planar circumcircle R shown here

$$\lambda = \cos^{-1}(R) \tag{14}$$

The cone angle is defined as the angle from the base to the surface of the cone. With this definition, a circular cone will always have a cone angle between 0 and  $\pi/2$  radians which matches the range of the arccos function in equation (14) for values of R between 0 and 1.

#### 3.2.3 Grashof conical developable mechanisms

Similar to cylindrical developable mechanisms, not all spherical mechanisms can be mapped to a conical surface in both open and crossed configurations. The method to determine the potential configuration also uses the Grashof condition, but additional considerations are required.

 Table 2
 A non-Grashof spherical mechanism whose three-dimensional quadrilateral satisfies the Grashof condition

Link angles (deg)	Spherical Grashof condition	3D quad leg lengths	Planar Grashof cond.	$R_{open}$	$R_{crossed}$
70	Non-Grashof	1.147	Grashof	0.90476	2.3064
80		1.286			
120		1.732			
40		0.684			

Notes: That the radius of the circumcircle of the crossed cyclic quadrilateral is greater than 1.

The previous section outlined how a planar cross-section can represent a conical developable mechanism. However, the resulting cyclic quadrilateral will not necessarily have the same Grashof condition as the spherical mechanism it represents. For example, a non-Grashof spherical mechanism may generate a set of link lengths that satisfy the

Grashof condition. From Subsection 3.1.2, it was shown that a set of links that satisfy the Grashof condition will have an open and crossed cyclic configuration.

With the presented case of a set of links from a non-Grashof spherical mechanism that satisfy the planar Grashof condition, the radius of the crossed cyclic quadrilateral will be greater than one. This R value is outside of the domain of equation (14), and no cone angle can be found. This is further verified by the fact that the vertices are all constrained on a unit sphere with radius of one, so it is not possible to make a cyclic quadrilateral whose circumcircle has a radius greater than one. Therefore, just as the case for planar four-bar mechanisms, a non-Grashof spherical mechanism can only conform to a conical surface with an open configuration. An example calculation is presented in Table 2.

For spherical Grashof mechanisms, the results are similar to planar Grashof mechanisms. For a non-folding spherical mechanism, there are two circular cones to which it can be mapped in an open or crossed configuration.

For a folding spherical mechanism, there will be one cone to which the mechanism can be mapped in an open configuration. If there are not two sets of equal link angles, the radius of the crossed cyclic quadrilateral will be one. Using equation (14), the resulting cone angle is zero which corresponds to a flat cone, or a single plane. A mechanism with two sets of equal link angles will not return a valid radius for a crossed configuration. However, just as in the case of the planar parallelogram and kite mechanisms, there exist a range of radii for crossed cyclic quadrilaterals. Instead of approaching infinity, the upper limit  $R_{\rm max}$  for the radius of this mechanism is one. The lower limit,  $R_{\rm min}$  is half the length of the side generated from the largest link angle,  $\phi_{\rm max}$ . This means that the range for cone angles will be between zero and  $\lambda_{\rm max}$ . Expressions for  $R_{\rm min}$  and  $\lambda_{\rm max}$  are

$$R_{\min} = \frac{1}{2}\sqrt{2 - 2\cos(\phi_{\max})}\tag{15}$$

$$\lambda_{\text{max}} = \cos^{-1}(R_{\text{min}}) \tag{16}$$

#### 4 Expanding existing mapping methods

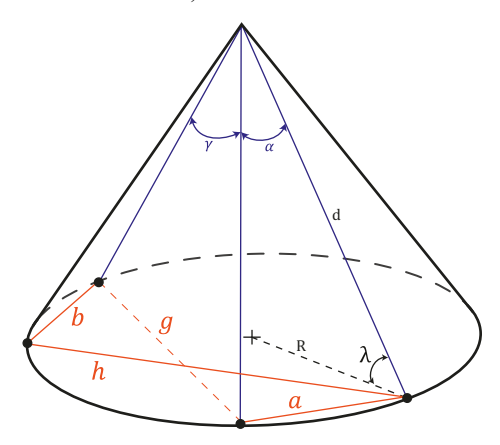
Two previous works have presented methods to determine the geometry of the developable surfaces needed to map planar or spherical four-bar mechanisms in a conformed position (Murray and McCarthy, 2020; Hyatt et al., 2020). Both methods determine the appropriate geometry by employing a numerical solution to different systems of equations. This section explores how each method can be expanded to apply to both cylindrical and conical developable mechanisms.

# 4.1 Adaptation of the coordinate method to conical developable mechanisms

The coordinate method, discussed in Subsection 2.4.1, maps planar mechanisms to cylindrical surfaces (Murray and McCarthy, 2020). While not explored in its original presentation, the system of equations [equation (6)] can be readily adapted to map spherical mechanisms to conical surfaces (determining the cone angle) using a planar cross-section of the conical surface, as shown below.

For a spherical mechanism with link angles  $(\gamma, \alpha, \eta, \beta)$ , equation (13) can be used to calculate the quadrilateral leg lengths which can be normalised to (g, a, h, b), respectively. When these parameters are used in equations (6), (7) and (8) the resulting circle is the circular cross-section of a cone at a distance d from the tip of the cone along the surface. Figure 9 shows some of these parameters on a conical section.

Figure 9 A conical diagram showing the parameters to numerically solve for the cone angle (see online version for colours)



Notes: Only two of the four link angles are shown for clarity  $(\gamma, \alpha)$ .

Any one of the spherical link angles and normalised leg lengths can be used to calculate the angle of the cone. If the length g = 1, the distance d based on the link angle  $\gamma$  is

$$d = \sqrt{\frac{1}{2(1 - \cos(\gamma))}}\tag{17}$$

Equation (17) can be used with the radius R calculated from equation (8) to calculate the cone angle  $\lambda$ .

$$\lambda = \cos^{-1} \frac{R}{d} \tag{18}$$

#### 4.2 Adaptation of the loop sum method to cylindrical developable mechanisms

The loop sum method, discussed in Subsection 2.4.2, maps spherical mechanisms to conical surfaces (Hyatt et al., 2020). This method can also be expanded to map planar mechanisms to cylindrical surfaces (determining the radius of the cylindrical reference surface), as discussed below.

Just as the projected angles are the angles between the vertices of a cyclic quadrilateral representing a conical developable mechanism, similar angles can be found for cylindrical developable mechanisms as shown by Greenwood et al. (2019). For a link length l, the central angle  $\psi_l$  about the circumcircle with radius R is

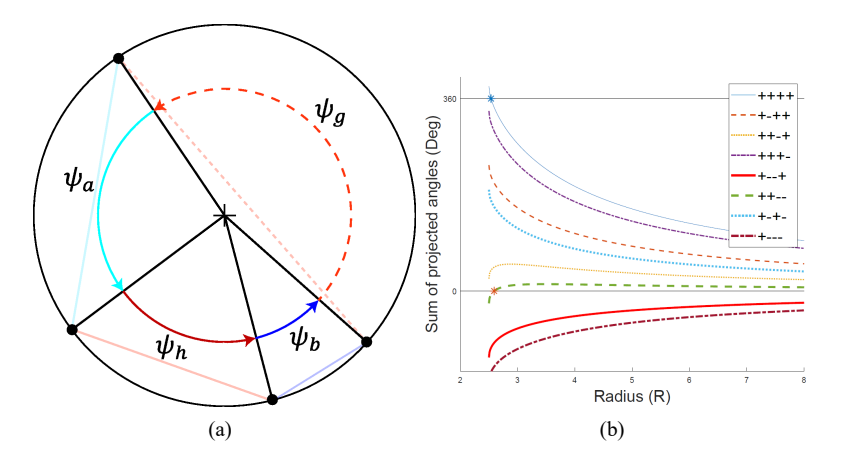
$$\psi_l = 2\sin^{-1}\left(\frac{l}{2R}\right) \tag{19}$$

For a cylindrical developable mechanism, the angles from each link will always sum to an integer multiple of 360° (Greenwood et al., 2019). Therefore, given a four-bar planar mechanism with links (g, a, h, b) with central angles  $(\psi_g, \psi_a, \psi_h, \psi_b)$  as seen in Figure 10(a) the following relationship exists

$$\pm \psi_a \pm \psi_a \pm \psi_h \pm \psi_b = 360k \tag{20}$$

This relationship is analogous to equation (10), however instead of an unknown cone angle, equation (20) yields 16 equations with an unknown radius. If at some radius, one of the equations is equal to a multiple of 360, that indicates the radius of the cylindrical surface to which the planar mechanism can be mapped. This is demonstrated by a Grashof mechanism with link lengths (4, 3, 5, 1) in Figure 10(b). The graph indicates that the mechanism can be mapped to two cylinders with radii of about 2.54 and 2.59 in an open and crossed configuration, respectively.

**Figure 10** (a) Central angles of the top mechanism in Figure 4 (b) Eight combinations of projected angles for a Grashof mechanism (see online version for colours)



Note: Two combinations cross a multiple of 360 indicating valid radii.

#### 4.3 Discussion of mapping methods

The coordinate method and loop sum method both yield the same results as the method using cyclic quadrilaterals (Section 3). There are certain advantages and disadvantages to each method. The major advantage of using the equations for cyclic quadrilateral is the ability to calculate an exact analytical solution without the use of a numerical solver. Equation (12) will yield the radius of the circumcircle of the open or crossed solution of a planar four-bar mechanism with only the four original link lengths. With the addition of equations (13) and (14), the same results can be found with just the link angles of a spherical mechanism. This can be useful in designing developable mechanisms where the link length ratios are fixed or if the radius of the cylinder is a design variable.

One advantage of the coordinate method is that by solving for the joint locations on the circumcircle, more information about the configuration of the mechanism can be quickly found such as the angles between the different links. When using equation (12),

only the radius is found, so further analysis is required to determine the location of the vertices on the surface.

All methods reach the same conclusion for Grashof and non-Grashof mechanisms: Grashof mechanisms can be mapped to two unique surfaces, while non-Grashof mechanisms only have one valid configuration. Through the use of equation (11), a mathematical explanation can be found from the principles of cyclic quadrilaterals. However, as explained in Subsection 3.1.3, using equation (12) with a folding mechanism may only result in a single solution when multiple may be possible. Using a numerical or graphical solution can result in finding all the potential solutions for a folding mechanism as demonstrated in Hyatt et al. (2020).

# 5 Cyclic quadrilaterals: application to intramobility and extramobility

Once a mechanism has been mapped to a developable surface, the location of the cyclic quadrilateral within the circumcircle can be used to understand the potential behaviours of the linkage such as intramobility and extramobility.

Greenwood et al. (2019) proposed a graphical method, called the shadow method, to determine if a cylindrical developable mechanism is capable of exhibiting extramobility and intramobility. This method can also be applied to conical developable mechanisms (Hyatt et al., 2020). The shadow method is applied by shading the region bounded by vectors of the two side links (b and d in a traditional four-bar mechanism) and contains the ground link and coupler. For a mechanism to exhibit purely extra and intramobile behaviour (i.e., no transmobile behaviour), the shaded region may not cover the centre of the circle.

The shadow method relies on the two side link vectors, which are equivalent to two opposite sides of a cyclic quadrilateral. Therefore, the shadow method is directly applicable to cyclic quadrilaterals. Hence, the cyclic quadrilaterals of both cylindrical and conical developable mechanism can be used to determine the behaviour (intramobile or extramobile) that the mechanism can exhibit.

#### 5.1 General cases

Assume four points are arbitrarily placed along the circumference of a circle where each point represents a vertex of a cyclic quadrilateral. With these four points, three possible cyclic quadrilaterals can be formed (one open and two crossed), as shown in Figure 11. There are two general cases: where the open configuration does not contain the centre of the circle and when it does (labeled here as cases 1 and 2, respectively). These cases and their corresponding cyclic quadrilaterals are shown in Table 3.

The motion of the mechanism, including extramobility and intramobility, depends on which link is the ground link. Hence, one of the sides of the cyclic quadrilateral must be chosen to represent the grounded link of a four-bar mechanism. Interestingly, the shadow method depends solely on which pair of links are the side links and which pair of links are the ground/coupler links. Therefore, only two subcases need be examined, one for each pair selected as the grounded/coupler pair. This is represented in Table 3 by columns A and B. The cyclic quadrilaterals in column A are identical to those in column B, except with a different link selected as the ground link.

Figure 11 (a) Four arbitrary points along the circumference of a circle (b) (c) (d) The three possible cyclic quadrilaterals that use the four points as vertices (see online version for colours)

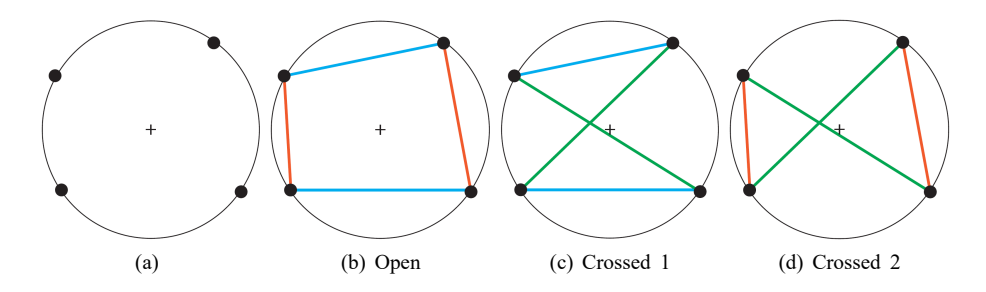
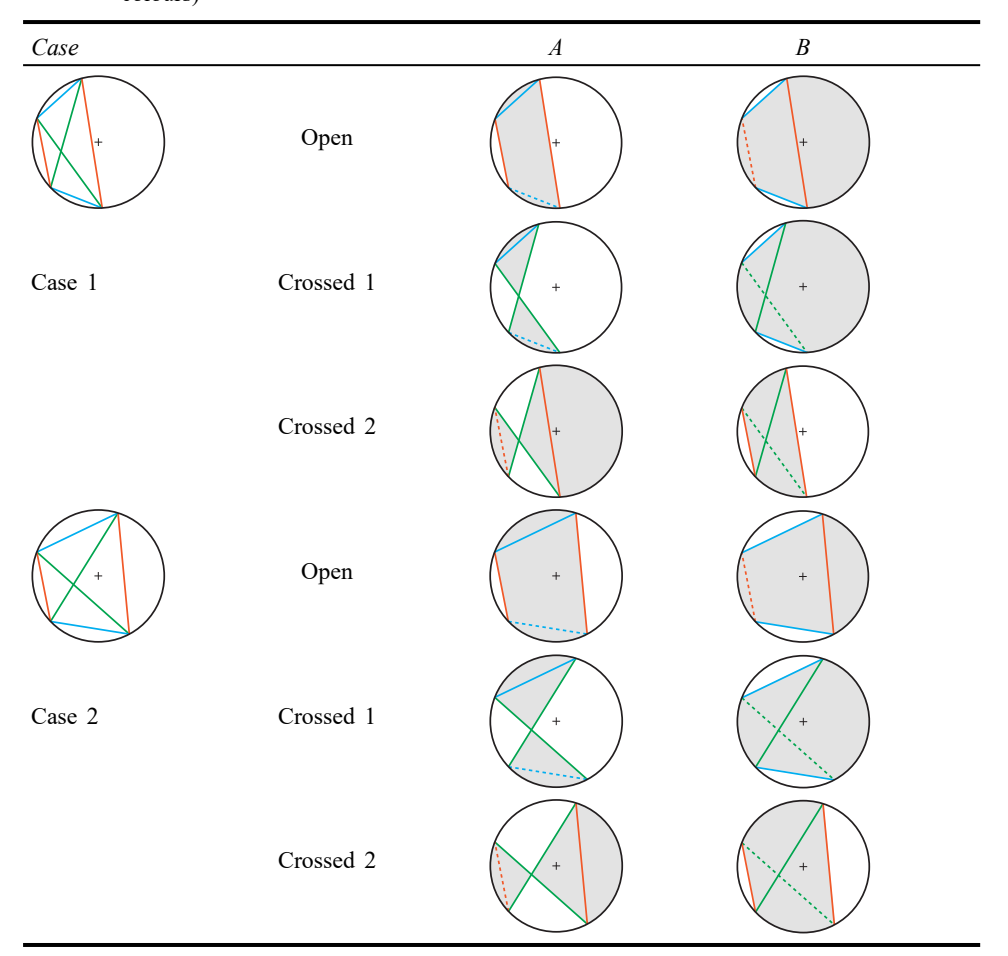


**Table 3** General cases of cyclic quadrilaterals and their capacity to generate extra and intramobile mechanisms (shown with the shadow method) (see online version for colours)



Notes: Mechanisms without the shaded region overlapping the centre of the circle can possibly be extra and intramobile. Dashed lines indicate the ground link.

Table 3 demonstrates the 12 possible cyclic quadrilaterals from four arbitrary points (six each for cases 1 and 2). It can be seen using the shadow method that a cyclic quadrilateral in case 1 is capable of producing three different mechanisms that can potentially demonstrate extramobile and intramobile behaviour (open A, crossed 1A, and crossed 2B). However, a mechanism in case 2 may only produce one mechanism that can potentially demonstrate extramobile and intramobile behaviour (crossed 1A).

#### 5.2 Special conditions

Special conditions exist in the event that a link within the cyclic quadrilateral intersects the centre of the circle. If one link extends halfway across the circle, the mechanism cannot exhibit intramobile behaviour (Greenwood et al., 2019).

Table 4 Summary of possible intramobile or extramobile behaviour for all cases in Table 3

Possible behaviour	Case 1					Case 2						
	Open		Crossed 1		Crossed 2		Open		Crossed 1		Crossed 2	
	A	В	$\overline{A}$	В	$\overline{A}$	В	$\overline{A}$	В	$\overline{A}$	В	$\overline{A}$	В
Intramobility	Y*	N	Y	N	N	Y*	N	N	Y*	N	N	N
Extramobility	Y	N	Y	N	N	Y	N	N	Y	N	N*	N

Notes: Y indicates yes and N indicates not possible.

The only condition for which case 1 can have a link intersect the centre of the circle is when this is caused by one of the outer links. In this scenario, both configurations open A and crossed 2B are now incapable of intramobile behaviour (but may still exhibit extramobile behaviour). There are no other changes for this special condition. Note that configuration crossed 1A can still exhibit both intramobile behaviour and extramobile behaviour, even if one of the outer links intersects the centre of the circle.

There are two special conditions that exist for case 2. The first is if one of the crossed links intersects the centre of the circle. If this occurs, configuration crossed 1A cannot exhibit intramobile behaviour. However, it is important to note that now configuration crossed 2A, which previously could not exhibit intramobile or extramobile behaviour, can now exhibit extramobile behaviour (in this special condition). There are no other changes for this first special condition.

The second special condition exists when both crossed links intersect the centre of the circle (this can only happen if the mechanism is a crossed parallelogram mechanism). Similar to above, in this condition, configurations crossed 1A and 2A can exhibit extramobile behaviour but cannot exhibit intramobile behaviour. It should be noted that these configurations may have extramobile motion in only one of the two directions of motion. For a link to extend through the middle of the circle, its actual link shape must extend at an arc length  $\pi R$  around the circle. While either direction may be used (link curving either direction around the circle), only one direction can be selected for extramobile motion. In other words, a link that extends halfway around the circle cannot be used to provide extramobile motion in both directions. Table 4 gives a summary of all of the cases with an asterisk indicating that the special condition will change the potential behaviour.

<sup>\*</sup>the possible behaviour changes if a link touches the centre of the circle.

#### 6 Discussion and conclusions

This paper explores three methods for mapping linkages to cylindrical and conical surfaces, thereby creating cylindrical and conical developable mechanisms.

The cyclic quadrilateral method provides advantages of both an analytical and graphical approach. The generalised equation for the radius of the circumcircle [equation (12)] provides a direct way to determine the radius of a cylindrical developable mechanism. This equation can be useful in designing developable mechanisms where the link length ratios are fixed or if the radius of the cylinder is a design variable. With equations (13) and (14) and (12) can also be used to find the cone angle for a conical developable mechanism. For example, the link lengths of a planar four-bar mechanism or the link angles of a spherical four-bar mechanism can be used to determine the geometry of the developable surface to which it can be mapped.

The use of cyclic quadrilaterals to analyse conical developable mechanisms is significant because designers can use a planar model to analyse a three-dimensional conical mechanism. As planar mechanisms are typically simpler to model and test than spherical mechanisms, this connection can offer an intuitive understanding of the complex motion. There are still limitations because even the Grashof condition may differ between the spherical mechanism and its planar counterpart as explained in Subsection 3.2.3. Nevertheless, the planar model can give an initial idea of how the mechanism will move with respect to the surface when near its conformed position. This work can lead to future research into using planar representations and projections to analyse conical developable mechanisms.

Two additional methods were also included, the coordinate method for conical developable mechanisms and the loop sum method for cylindrical developable mechanisms. These were expanded from previous work and now can be applied to map mechanisms to both cylindrical and conical surfaces.

Beyond the presentation of the mapping methods, a number of useful principles have been identified. Specifically, four-bar mechanisms can be mapped to regular cylindrical or circular conical surfaces, regardless of their Grashof condition. However, only Grashof mechanisms can be mapped to these surfaces in a crossed configuration. Therefore, the only way to map a non-Grashof mechanism to a regular cylindrical or circular conical surface is in its open configuration. It follows that forming any four-bar mechanism from a crossed cyclic quadrilateral forces the mechanism to be a Grashof mechanism, regardless of any other geometrical considerations. Any developable mechanism in a crossed configuration can be identified as a Grashof mechanism without any calculations.

It can observed from Table 3 that the only way to create an open-loop mechanism that achieves extra or intramobile behaviour is through case 1, open A. All other cases of convex quadrilaterals result in exclusively transmobile behaviour. This is significant because it has been established that non-Grashof mechanisms can only have convex cyclic quadrilateral configurations. Therefore, the only way to have a non-Grashof mechanism that can exhibit extramobile or intramobile behaviour must belong to case 1, open A. Furthermore, this means that for non-Grashof mechanisms desiring intramobile and extramobile behaviour, all vertices must lie on one half of the circumcircle. Table 3 also demonstrates that all other cases of mechanisms that can exhibit extramobile or intramobile behaviour are necessarily Grashof mechanisms.

The methods, equations, and analysis presented in this paper provide useful tools in the design of cylindrical and conical developable mechanisms. The analytical nature of the included equations builds on previous work and is useful when numerical solutions are needed. Much of this work also employs graphical analysis, which can be very advantageous and lend to the designer's intuition rather than solely an equation-based analytical method.

#### References

- Andreescu, T. and Enescu, B. (2011) *Mathematical Olympiad Treasures*, Springer Science & Business Media, Basel, Switzerland.
- Atzema, E.J. (2015) 'From Brahmagupta to Euler: on the formula for the area of a cyclic quadrilateral', *BSHM Bulletin: Journal of the British Society for the History of Mathematics*, Vol. 30, No. 1, pp.20–34, DOI: 10.1080/17498430.2014.942818.
- Bowman, F. (1952) 'The plane four-bar linkage', *Proceedings of the London Mathematical Society*, Vol. 2, No. 1, pp.135–146.
- Butler, J., Greenwood, J., Howell, L. and Magleby, S. (2020) 'Limits of extramobile and intramobile motion of cylindrical developable mechanisms', *Journal of Mechanisms and Robotics*, In Review.
- Caymaz, G.F.Y., Yardımli, S., Turan, B.O. and Tarim, A. (2018) 'Wooden structures within the context of parametric design: pavilions and seatings in urban landscape', *Journal of Architectural Research and Development*, Vol. 2, No. 3, pp.34–54.
- Chiang, C.H. (2000) Kinematics of Spherical Mechanisms, Krieger Pub., Malabar, Florida, USA.
- Fraivert, D., Sigler, A. and Stupel, M. (2019) 'Necessary and sufficient properties for a cyclic quadrilateral', *International Journal of Mathematical Education in Science and Technology*, pp.1–26, DOI: 10.1080/0020739X.2019.1683772.
- Gavriil, K., Schiftner, A. and Pottmann, H. (2018) 'Optimizing B-spline surfaces for developability and paneling architectural freeform surfaces', *CAD Computer Aided Design*, Vol. 111, pp.29–43, arXiv:1808.07560, DOI: 10.1016/j.cad.2019.01.006.
- Grashof, F. (1883) in Voss, L. (Ed.): Theoretische Maschinenlehre: Bd. Theorie der Getriebe und der Mechanischen Messinstrumente, Vol. 2.
- Greenwood, J.R., Magleby, S.P. and Howell, L.L. (2019) 'Developable mechanisms on regular cylindrical surfaces', *Mechanism and Machine Theory*, December, No. 142, p.103584.
- Gupta, R.C. (1977) 'Parameśvara's rule for the circumradius of a cyclic quadrilateral', *Historia Mathematica*, Vol. 4, No. 1, pp.67–74.
- Hyatt, L.P., Magleby, S.P. and Howell, L.L. (2020) 'Developable mechanisms on right conical surfaces', *Mechanism and Machine Theory*, Vol. 149, p.103813, DOI: 10.1016/j.mechmachtheory.2020.103813.
- Josefsson, M. (2017) '101.38 metric relations in crossed cyclic quadrilaterals', *The Mathematical Gazette*, Vol. 101, No. 552, pp.499–502.
- Josefsson, M. (2019) 'More characterizations of cyclic quadrilaterals', *International Journal of Geometry*, Vol. 8, No. 2, pp.14–32.
- Lawrence, S. (2011) 'Developable surfaces: their history and application', *Nexus Network Journal*, Vol. 13, No. 3, pp.701–714.
- Lim, J.J. and Erdman, A.G. (2003) 'A review of mechanism used in laparoscopic surgical instruments', *Mechanism and Machine Theory*, Vol. 38, No. 11, pp.1133–1147.
- Liu, Y.J., Tang, K., Gong, W.Y. and Wu, T.R. (2011) 'Industrial design using interpolatory discrete developable surfaces', *CAD Computer Aided Design*, Vol. 43, No. 9, pp.1089–1098.

- Martín-Pastor, A. (2019) 'Augmented graphic thinking in geometry. Developable architectural surfaces in experimental pavilions', in *Graphic Imprints*, EGA 2018, pp.1065–1075, Springer International Publishing, Alicante, Spain.
- McCarthy, J.M. and Soh, G.S. (2010) Geometric Design of Linkages, Vol. 11, Springer Science & Business Media, New York, USA.
- Murray, A. and McCarthy, J.M. (2020) Computation of the Developable Form of a Planar Four-Bar Linkage, pp.172–178, Springer, Cham, DOI: 10.1007/978-3-030-43929-3\_16.
- Nelson, T.G., Zimmerman, T.K., Lang, R.J., Magleby, S.P. and Howell, L.L. (2019) 'Developable mechanisms on developable surfaces', Science Robotics, Vol. 4, No. 27, p.5171.
- Seymour, K., Sheffield, J., Magleby, S.P. and Howell, L.L. (2019) 'Cylindrical developable mechanisms for minimally invasive surgical instruments', in *Proceedings of the ASME Design Engineering Technical Conference*, American Society of Mechanical Engineers (ASME), Vol. 5B-2019.
- Usiskin, Z. (2008) The Classification of Quadrilaterals: A Study in Definition, IAP.